The Thesis Committee for Jonathan David Pantano Certifies that this is the approved version of the following Thesis:

Assessing Linkages between Climate Teleconnections and Freshwater Inflows to Texas Bays and Estuaries

APPROVED BY

SUPERVISING COMMITTEE:

Bridget R. Scanlon, Supervisor

Jean-Philippe Nicot

Suzanne A. Pierce

Assessing Linkages between Climate Teleconnections and Freshwater Inflows to Texas Bays and Estuaries

by

Jonathan David Pantano

Thesis

Presented to the Faculty of the Graduate School of

The University of Texas at Austin

In Partial Fulfillment

Of the Requirements

For the Degree of

Master of Science in Energy and Earth Resources

The University of Texas at Austin

May 2022

Abstract

Assessing Linkages between Climate Teleconnections and Freshwater Inflows to Texas Bays and Estuaries

by

Jonathan Pantano, MSEER

The University of Texas at Austin, 2022

SUPERVISOR: Bridget R. Scanlon

Understanding spatiotemporal variability in freshwater inflows to the bays and estuaries along the Gulf of Mexico is critical for water resources management to maintain the health of the ecosystem and marine life. The objective of this study was to assess linkages between climate teleconnections (e.g. El Nino Southern Oscillation [ENSO], North Atlantic Oscillation [NAO], and Pacific Decadal Oscillation [PDO]), precipitation, and freshwater inflows to the Gulf of Mexico. Seasonal Trend Decomposition using LOESS (STL) analysis was used to decompose monthly precipitation and freshwater inflows (1941-2015) to each bay and estuary, isolating long-term variability, and comparing it to ENSO during warm and cool PDO phases and NAO.

Results show that there are moderately strong positive correlations between ENSO and precipitation (R = 0.37 to 0.7) with mostly higher precipitation during El Nino

and lower precipitation during La Nina. These correlations were weakened during PDO warm phase (R = 0.16 to 0.41) and amplified during PDO cool phase (R = 0.66 to 0.8). Temporal variability in precipitation was linked to bay and estuary freshwater inflows, showing high flows during El Nino and low flows during La Nina. Additionally, there are moderately strong positive correlations between NAO and freshwater inflows to two of the 10 bays/estuaries in the northeast (Sabine-Neches and Trinity San Jacinto, R = 0.45 and 0.41). These correlations tend to occur within the year of the driving conditions in the Pacific and Atlantic oceans. Identifying these linkages and the corresponding response times can help predict and manage the hydrologic response to wet and dry climate cycles linked to climate teleconnections along the Texas Gulf Coast to help protect and maintain the health of the vital estuarine environments.

Table of Contents

List of Tables

List of Figures

List of Acronyms

MAP	Mean Annual Precipitation
PPT	Precipitation
FWI	Freshwater Inflows
STL	Seasonal Trend Decomposition using LOESS
ENSO	El Niño-Southern Oscillation
PDO	Pacific Decadal Oscillation
NAO	North Atlantic Oscillation

1. Introduction

The Texas Gulf coast, extending southwest from Louisiana to the U.S.-Mexico border, contains ~3,400 km of the bay-estuary-lagoon shoreline [1]. This shoreline is divided into seven major and five minor estuaries (only three minor estuaries will be used in this research due to lack of data), which are fed by 15 major river systems in Texas [1]. These estuaries provide both economically and ecologically important resources to the state. Like all estuaries, freshwater inflows are vital in maintaining proper levels of salinity, nutrients, and sediments, which sustain the estuarine ecosystem. Freshwater inflows, whether from surface water or precipitation, are controlled by both the hydrologic cycle and human water resource management [2].

Most Texas estuaries are comprised of several shallow (between 1-4 m depth) bays in a primary-secondary (sometimes tertiary) relationship. The bays are typically protected from the Gulf of Mexico via barrier islands and the estuarine environment is created through channels that allow saltwater from the Gulf to mix with the freshwater inflows from the bays [3]. Despite their physical similarities, estuaries are hydrologically diverse because of the climatic gradient that influences the hydrologic cycle. Precipitation gradually decreases along the coast from the Louisiana border (mean annual precipitation (MAP), 1,420 mm) to the southwest (MAP, 690 mm) [1].

Freshwater inflows also decline along the climatic gradient from northeast to southwest, with an annual average of ~16 km^3 emptying into the Sabine-Neches estuary compared to less than 1 km^3 for Laguna Madre estuary to the south. In addition to the northeast-southwest spatial variation in freshwater inflows, temporal variations in inflows are linked to precipitation and climate variability. For example, a ten-year drought during the

late 1940s and continuing into the 1950s in Texas resulted in river inflows that were 86% below the average [4]. This severe drop in freshwater inflows to the estuaries had a significant negative impact on the Gulf fisheries and marine life [4]. Climate teleconnections (e.g., El Nino Southern Oscillations (ENSO), North Atlantic Oscillations (NAO), and Pacific Decadal Oscillations (PDO)), and related atmospheric-ocean coupling mechanisms can also affect freshwater inflows and the health of the Texas estuaries.

The main driver of monthly SSTs in the Central Pacific Ocean is ENSO. ENSO is generally considered as having three phases; neutral, warm and cold that occur in 2–7-year cycles. During the neutral phase, warm air and surface water are blown west via east to west blowing trade winds which keep the central Pacific cool. Positive (warm phase) of ENSO (El Niño) occurs when the trade winds weaken or reverse, resulting in warm air and surface water moving to the central Pacific or towards the eastern Pacific. Negative (cool) phase (La Niña) occurs when the trade winds are blowing east to west, as normal, but strengthen with warm air and surface water becoming trapped in the western Pacific. El Niño (La Niña) events have been linked to wetter (drier) conditions in the southwest and central regions of the United States, with opposite conditions in the northwest [5]. Precipitation and streamflow increased during warm phases of ENSO while droughts are more prevalent during cool phases of ENSO in the southwest/southcentral U.S. These effects are amplified when ENSO and PDO are in phase, with the frequency and strength of warm and cold ENSO phases increasing when PDO is in the same phase (Figure 1) [5-7].

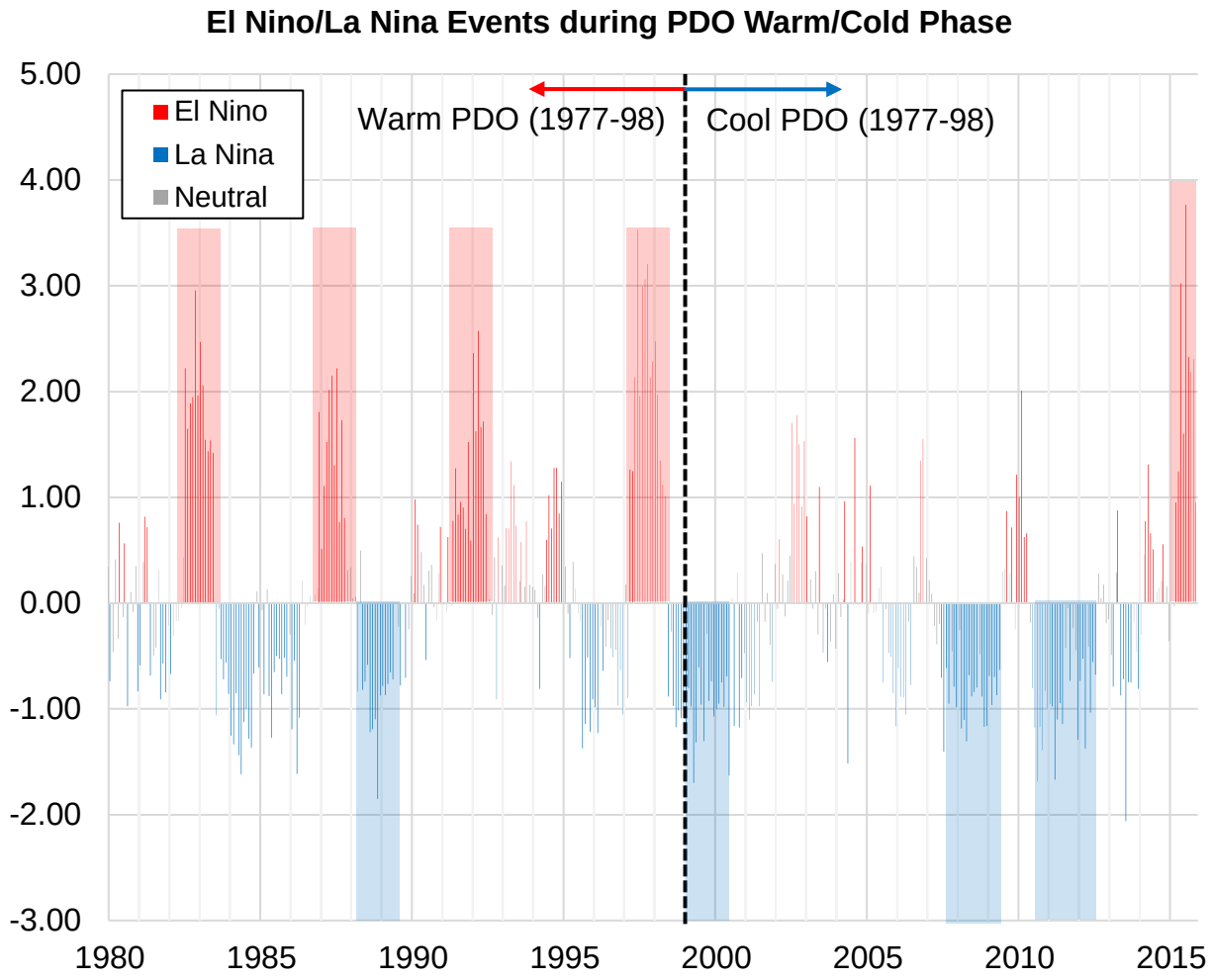

Figure 1 The red, shaded regions indicate strong El Niño events (sustained index values >1) while the blue shaded regions show stronger La Niña events (sustained index values <-1), From 1977 to 1998, PDO was in a warm phase and there were four strong El Niño events, compared to one strong event in the roughly 20 years since the phase change. Similarly, there have been four strong La Niña events after the shift to a PDO cool phase in 1999, compared to one during the PDO warm phase.

The main driver of monthly SST variations in the North Pacific Ocean, from 20°N poleward, is the PDO index [8]. The PDO has two phases: warm and cold and each phase lasts for 20-30 years, requiring 40-60 years for a full cycle. Positive values of PDO (warm phase) are related to below average sea level pressures in the North Pacific, cool SSTs in the interior, and warm SSTs along the Pacific Coast [9]. Negative values of PDO (cold phase) occur when these conditions are opposite.

Over the Atlantic Ocean, the North Atlantic Oscillation (NAO) is a north-south, dipole pattern centered near Greenland [10]. NAO is characterized by patterns in SSTs and sea level pressure from high latitudes near Greenland and Iceland (sub-polar low) to the central Atlantic (subtropical high) [11]. Positive values of NAO (warm phase) are related to higher than average values for the sub-polar low and sub-tropical high, creating a stronger Atlantic jet stream that shifts the storm track north. Negative values of NAO (cold phase) are related to the opposite conditions [12].

Fluctuations in the NAO have been linked to climate variability in the United States, with impacts observed along the east coast. A NAO warm phase is associated with mild late-winter temperatures while an NAO cold phase leads to cooler temperatures [12]. Statistically significant links between precipitation and snowfall have also been observed when NAO is in a cold phase, although no significant link has been found between precipitation and the warm phase [13, 14]. The links between temperature and NAO have also been observed with a time lag in the southern portions of the western and central United States. Myoung and Lee et al. (2015) showed that temperature connections in late winter/early spring (Mar-Jun) in the southwest and south-central U.S. are strongly connected to NAO variability, with the connection strengthening since

1980, surpassing the strength of the temperature-PDO/ENSO relationship in these regions [15].

Climate teleconnections to hydrology have also been observed at the state and regional level. Murgulet et al. (2017) and Hergert (2015) showed that there was a strong correlation between PDO/ENSO and precipitation/streamflow in South Texas and the Rio Grande Valley. Correlations between PDO/ENSO have also been found in precipitation and streamflow for Central Texas and the Hill Country in all seasons except fall [16, 17]. Looking specifically at the estuaries, Tolan (2007) identified links between climate variability and salinity levels in the seven major estuaries of Texas. Inferences could be made on the effect of freshwater inflows based on salinity levels, although they were not explicitly stated [1]. Evaluating individual estuaries, a 2011 study found links between climate variability and macrofauna populations in the Lavaca-Colorado Estuary [2]. Macrofauna populations are influenced by several factors, such as temperature and salinity, and could indirectly be linked to a change in freshwater inflows.

Maintaining the health of Texas bays and estuaries is vital to the Texas economy. About 95% of the Gulf's recreationally and commercially important marine life species rely on the bays and estuaries during their life cycle [18]. Seagrass growth, which relies on salinity zones controlled by freshwater inflows, provides vital nurseries for various fish and shellfish and seafood caught and sold from the Gulf, is valued at $150-250 million annually. In addition to commercial seafood, recreational fishing along the coast generates over $2 billion a year. Finally, coastal tourism has helped make tourism the

third largest industry in Texas after oil and gas and agriculture, generating ~ $5.4 billion annually [19].

The objective of this research was to examine the linkages between the climate teleconnections and the hydrological variations in Texas estuaries (freshwater inflow and precipitation). Previous studies have found links between climate variability and precipitation patterns or other estuary characteristics, such as salinity or microfauna growth, as well as links between streamflow and discharges across the state. This study intends to look specifically at the freshwater inflows that feed directly into the bay and estuaries to determine if there is a linkage with precipitation and climate variability. This study includes a much longer time period (1979 to 2021; 42 yrs.) than was available for previous studies. This study has implications for water management concerning the identifiability of the linkages of the local freshwater inflow and precipitation and regional climate change that could help to modify and develop better forecast strategies to maintain minimum flow levels and protect the health of estuarine environments.

2. Study Areas

2.1. Study Area Descriptions

The 10 estuaries used in this research, listed from east to west, are: Sabine-Neches, Trinity-San Jacinto, Brazos River, San Bernard and Cedar Lakes Complex, East Matagorda, Lavaca-Colorado, Guadalupe, Mission-Aransas, Nueces, and Laguna Madre (Figure 2). Two minor estuaries, Christmas Bay and Rio Grande, were not included due to the unavailability of data.

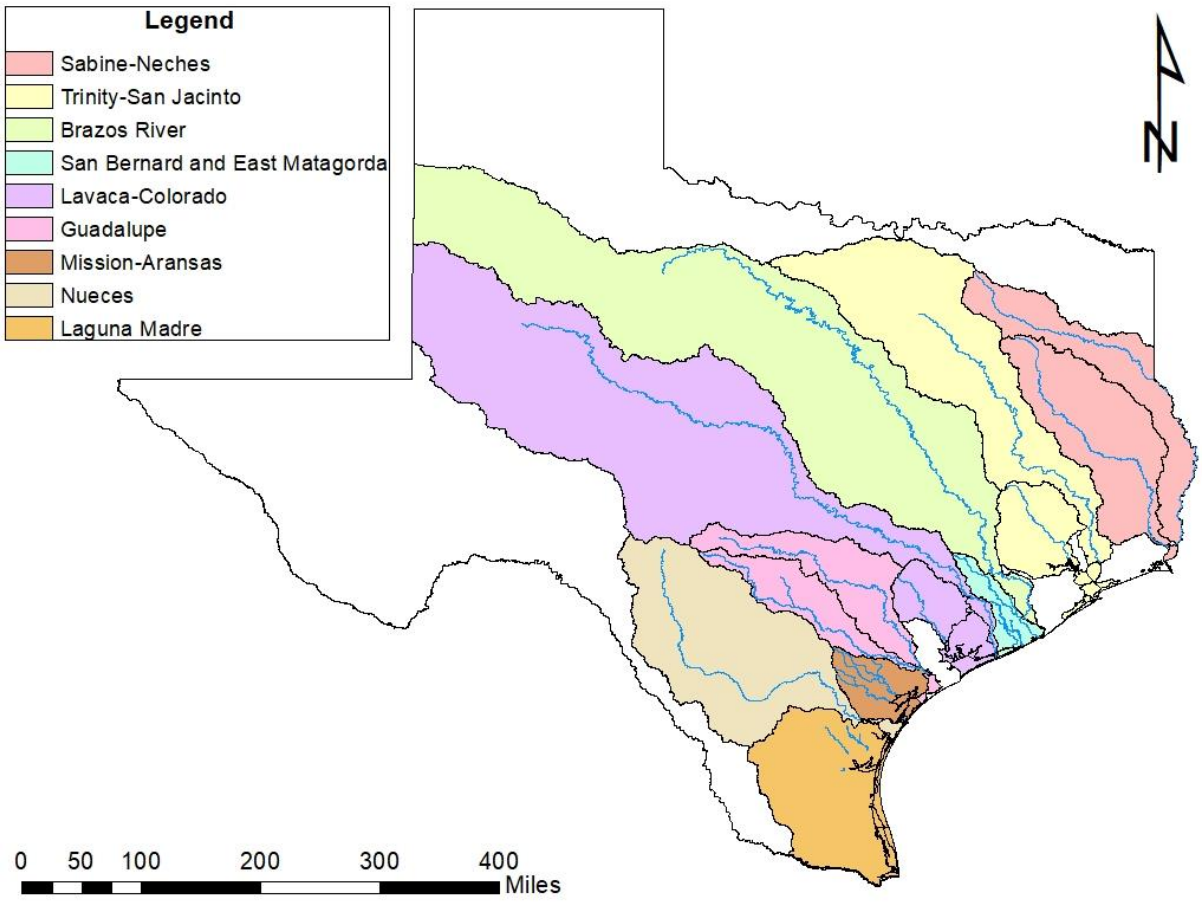

Figure 2. Map showing each of the ten estuaries with the river basins from which they receive their FWIs. GIS data files retrieved from the Texas Water Development Board, https://www.twdb.texas.gov/mapping/gisdata.asp.

2.1.1. Sabine-Neches Estuary

The Sabine-Neches Estuary is located at the Texas and Louisiana border and connected to the Gulf of Mexico via Sabine Pass. The estuary receives freshwater inflows from the Sabine and Neches River Basins and from a portion of the Neches-Trinity Coastal Basin. In addition to the seven-mile-long Sabine Pass, the estuary also includes Sabine Lake and the Sabine-Neches and Port Arthur Canals. Dredging of Sabine Pass has allowed salt-water intrusion to reach the lower portions of the Sabine and Neches Rivers, making these portions of the rivers and Sabine Lake nonpotable but still available for use by the industrial sector. However, the confluence of freshwater inflows and saltwater from the Gulf of Mexico supports a diverse ecosystem of fresh and salt marshes and is an important habitat for fish and shellfish while providing commercial and sport fishing opportunities for the public [20].

Wetland ecosystems that thrive in the estuary are reliant upon the salinity gradient of Sabine Lake, with economically and ecologically valuable plant, fish, and shellfish species requiring a mix of low-salinity, brackish, and saltwater habitats. In comparison to the other major Texas estuaries, the Sabine-Neches is the smallest at ~243 km^2 but receives one of the highest annual freshwater inflows. The most recent freshwater inflow study conducted in 2005 recommended an annual, seasonal inflow of 11.84 km^3 to maintain an ideal salinity gradient [21].

2.1.2. Trinity-San Jacinto Estuary

The Trinity-San Jacinto Estuary, commonly referred to as Galveston Bay, is made up of Galveston, Trinity, and East, and West Bays and is located southwest of the Sabine-Neches Estuary. The Trinity River, San Jacinto River, and Buffalo Bayou provide most

of the freshwater inflows into Galveston Bay, with smaller streams and bayous accounting for the remainder. Three channels connect the bay to the Gulf of Mexico and create the estuarine environment. The main channel, Bolivar Roads, connects directly to the bay while Rollover Pass and San Luis Pass connect the Gulf to East and West Bays, respectively [22].

At ~1402.5 km^2, the Trinity-San Jacinto Estuary is the largest in Texas and is the primary surface water resource for the Houston metropolitan and surrounding areas in the Texas Regional Water Plans. Because of its importance to regional water planning and the destination for flows from five basins, an annual average of 0.35 km^3 of inflows is diverted for uses in a variety of sectors while 0.55 km^3 of average annual return flows support the estuary [23]. On average, the annual inflow of 13.94 km^3 is far higher than the 2012 recommended inflow range of 5.18-6.41 km^3.

2.1.3. Colorado-Lavaca Estuary

Lavaca Bay, Matagorda Bay, Carancahua Bay, Tres-Palacios Bay, and a number of smaller bays make up the Matagorda Bay system, formally the Colorado-Lavaca Estuary. Covering ~912 km^2, it is the second largest estuary in Texas after the Trinity-San Jacinto Estuary and is fed primarily by the Colorado, Lavaca, and Tres Palacios Rivers. The Colorado-Lavaca Estuary connects directly to the Gulf of Mexico via two channels, the Entrance Channel and the Pass Cavallo [24].

Understanding, managing, and forecasting freshwater inflows is extremely important to the estuary to protect the ecosystem that relies on seasonal salinity fluctuations. This habitat promotes strong populations of shrimp, fisheries, and oyster beds, which are both ecologically and economically vital, with sport fishing and seafood harvests

accounting for ~$175 million annually [25]. The most recent freshwater inflow needs study for the estuary recommends annual inflows of roughly 3.45 km^3 [26]. The estuary is considered healthy, with the most recent coastal hydrology reporting an average of 4.3 km^3 of freshwater inflows annually, eclipsing the recommended total[24] [24, 27] [24] [25].

2.1.4. Guadalupe Estuary

Located adjacent to the Colorado-Lavaca Estuary, the Guadalupe Estuary comprises the San Antonio Bay, Hynes Bay, Guadalupe Bay, and Mesquite Bay. Unlike most of the other major Texas estuaries, the Guadalupe Estuary does not directly connect to the Gulf of Mexico. Saltwater intrusion occurs indirectly to the north, through the Pass Cavallo in the Colorado-Lavaca Estuary, and to the south via the Lydia Ann Channel in the Mission-Aransas Estuary. Freshwater inflows primarily come from the Guadalupe and the San Antonio rivers, which connect to the Guadalupe just north of the estuary [27]. A small estuary when compared to the others, it covers ~ 550.77 km^2 and remains relatively shallow throughout, with an average depth of 1 m. The estuary relies heavily on wind and freshwater inflows to cycle water due to the lack of a direct channel to the Gulf, and it receives roughly 2.47 km^3 of inflows annually [28].

The Guadalupe Estuary might be one of the most ecologically important estuaries in Texas. The high freshwater inflows, low tidal variations, and indirect access to the Gulf create a lower-salinity ecosystem that is an ideal habitat for marine life, such as blue crabs, oysters, shrimp, and various species of fish [29]. The fauna found in and around the estuary, specifically the blue crabs, make up a significant portion of the whooping

crane's diet and the only natural, migratory population of whooping cranes have established their wintering grounds within the Guadalupe Estuary.

2.1.5. Missions-Aransas Estuary

The Missions-Aransas Estuary comprises seven total bays and covers ~577 km^2. San Jose Island serves as a barrier island between the Gulf of Mexico and the estuary, but there are still direct connections at Cedar Bayou and Aransas Pass. Additionally, connections to the Guadalupe estuary to the north and the Nueces Estuary to the south allow for further saltwater intrusions. As is typical in estuaries, the Missions-Aransas Estuary is relatively shallow, with an average depth ranging from 0.6 to 2.6m [30]. The upstream drainage area for the Missions-Aransas is the smallest of the major Texas estuaries, and as such, a large portion of freshwater comes from direct precipitation over the bays. The remainder comes primarily from the estuary's namesake rivers, the Mission and Aransas rivers. Neither river is used as a surface water resource, and they flow to the estuary in their entirety. These rivers provide a low annual average of ~0.18 km^3/yr of freshwater inflows due to their small size and upstream drainage areas [31]. Despite the relatively low freshwater inflows, on average, the estuary still exceeds the recommended annual inflows of 0.07-0.11 km^3.

2.1.6. Nueces Estuary

Located south of the Mission-Aransas Estuary, The Nueces Estuary covers ~634.55 km^2 and includes the Nueces River (downstream from the Calallen Diversion Dam), the Corpus Christ, Nueces, Oso, and Redfish bays, and the Nueces Delta [32]. The primary source of freshwater inflows comes from the Nueces River, providing a mean annual inflow of 0.72 km^3.

Diversions from the Nueces River for municipal purposes led to the construction, improvement, and raising of several dams and reservoirs, which served to reduce freshwater inflows by ~50% over the course of previous decades. The estuary is in a climate zone with much higher evaporation than precipitation, and coupled with the declining freshwater inflows, created a hypersaline environment within the bay systems. Economically important marine life, such as shrimp and oysters, could not survive in these environments and significant legislation has improved the freshwater inflows into the estuary [32]. Additionally, intrabasin transfers have allowed return flows to the Nueces without the corresponding diversions, a huge benefit to the net inflows to the estuary [33].

2.1.7. Laguna Madre Estuary

The most southern of Texas' major estuaries, the Laguna Madre is split into two segments, the Upper Laguna Madre to the north and the Lower Laguna Madre to the south with the Saltillo Flats, a non-contributing land mass, in between. The Upper Laguna Madre is made up of Baffin and Corpus Christi Bays and receives freshwater inflows from the San Fernando Creek, while the Lower Laguna Madre does not connect to any bays nor does it receive inflows from the Rio Grande, despite its proximity to the U.S.-Mexico border. Freshwater inflows into the Lower Laguna Madre come from the Arroyo Colorado. The only direct connections to the Gulf of Mexico occur in the Lower Laguna Madre via the Port Mansfield Channel and the Brazos-Santiago Pass [34].

The Laguna Madre Estuary covers ~1,137.17 km^2 with an average depth of roughly 1.4 m and is considered a unique hypersaline environment. Both the Upper and Lower Laguna Madre estuaries have relatively low freshwater diversions for municipal

purposes, resulting in an average annual freshwater inflow of ~0.92 km^3. However, the evaporation rate is more than double the rate of precipitation and exceeds the sum of freshwater inflows and precipitation totals, resulting in an average negative freshwater balance of ~-0.68 km^3 [35].

2.1.8. Minor Estuaries

Texas recognizes five minor estuaries, although data are only available for three: Brazos River Estuary, San Bernard River and Cedar Lakes Estuary, and East Matagorda Bay. Minor estuaries in this study are located between the major estuaries of Trinity-San Jacinto to the north and Colorado-Lavaca to the south and run generally southwest along the coast, with the Brazos River Estuary to the north, followed by the San Bernard Estuary, and the East Matagorda Bay in the south.

The Brazos River flows directly into the Gulf of Mexico, creating an estuarine environment where freshwater and saltwater mix. The Brazos River Estuary is within two water planning regions, with diversions occurring for multiple industrial and municipal purposes. Despite the diversions, the estuary still receives annual freshwater inflows of ~7.82 km^3 [36].

The San Bernard River and Cedar Lakes Estuary includes Cowtrap Lake and Cedar Lakes, covering ~15.22 km^2 with an average depth of ≤ 1 m. The San Bernard River flows directly into the Gulf of Mexico, and the saltwater and freshwater mix, as well as inlets between the Gulf and Cedar Lakes, creating an estuarine environment. The estuary receives average annual freshwater inflows of ~ 0.84 km^3 and is affected by three planning regions [37].

East Matagorda Bay is unique among the major and minor estuaries as it does not have any direct freshwater inflows from rivers, creeks, or streams. Average annual freshwater inflows of ~0.66 km^3 are estimated from runoff models given that the Bay receives all of its freshwater inputs from direct precipitation or runoff from surrounding coastal basins. Covering 153 km^2 with an average depth of ~1 m, the bay becomes an estuary due to the influx of saltwater from the Gulf of Mexico via Mitchell's Cut [24, 38].

3. Materials and Methods

Linkages between global teleconnections and bay and estuary precipitation and freshwater inflows will be identified by looking at relationships between monthly time series data. A seasonal-trend decomposition will be applied to hydrology data and climate indices and the long-term variability will be cross-correlated using a time lag. The following sections will describe the datasets and methods that were used to identify these relationships.

3.1. Data

3.1.1. Precipitation

Precipitation data were retrieved from the Parameter-elevation Regressions on the Independent Slopes Model (PRISM) Climate Group [39]. The PRISM method, developed in 1991 by Oregon State University to generate gridded estimates of precipitation using multiple datasets and digital elevation models, typically at 4 km grid resolution [40]. The central coordinates of the 10 bays and estuaries were used as the location for the PRISM data. Monthly data were retrieved from 1948 through 2015.

3.1.2. Freshwater inflows

Freshwater inflows data were retrieved for each bay and estuary from the Texas Water Development Board (https://waterdatafortexas.org/coastal/hydrology). With no sited gauges where the inflow streams meet the bays or estuaries, the TWDB models outflows using both gauged and ungauged flows in each watershed. Ungauged flows are estimated using a rainfall-runoff simulation based on watershed precipitation, freshwater diversions for use by various sectors, and return flows. These ungauged

flows are added to the gaged flows from the 39 USGS streamflow gages within the watersheds to estimate the flows into the bay and estuaries.

Each bay and estuary had monthly outflow data from 1948 through 2015, with the exception of the minor estuaries, with coverage from 1979 through 2015. The long-term variabilities for each dataset were generated for the entire time series and were then truncated to different date ranges corresponding to the climate indices to allow for comparison. The long-term variability for the climate indices were truncated to fit the shorter data window for the minor estuaries.

3.1.3. Climate indices

3.1.3.1. El Niño Southern Oscillation (ENSO) Index

This study uses the monthly ENSO index values derived from precipitation patterns in the Pacific to monitor and describe ENSO events [41]. The monthly index covers the period from 1979 to the present (Figure 3). Time series data for 1979-2021 were retrieved for the study from NOAA Physical Science Laboratory (Retrieved from https://psl.noaa.gov/data/climateindices/list/#. Accessed 14 January 2022).

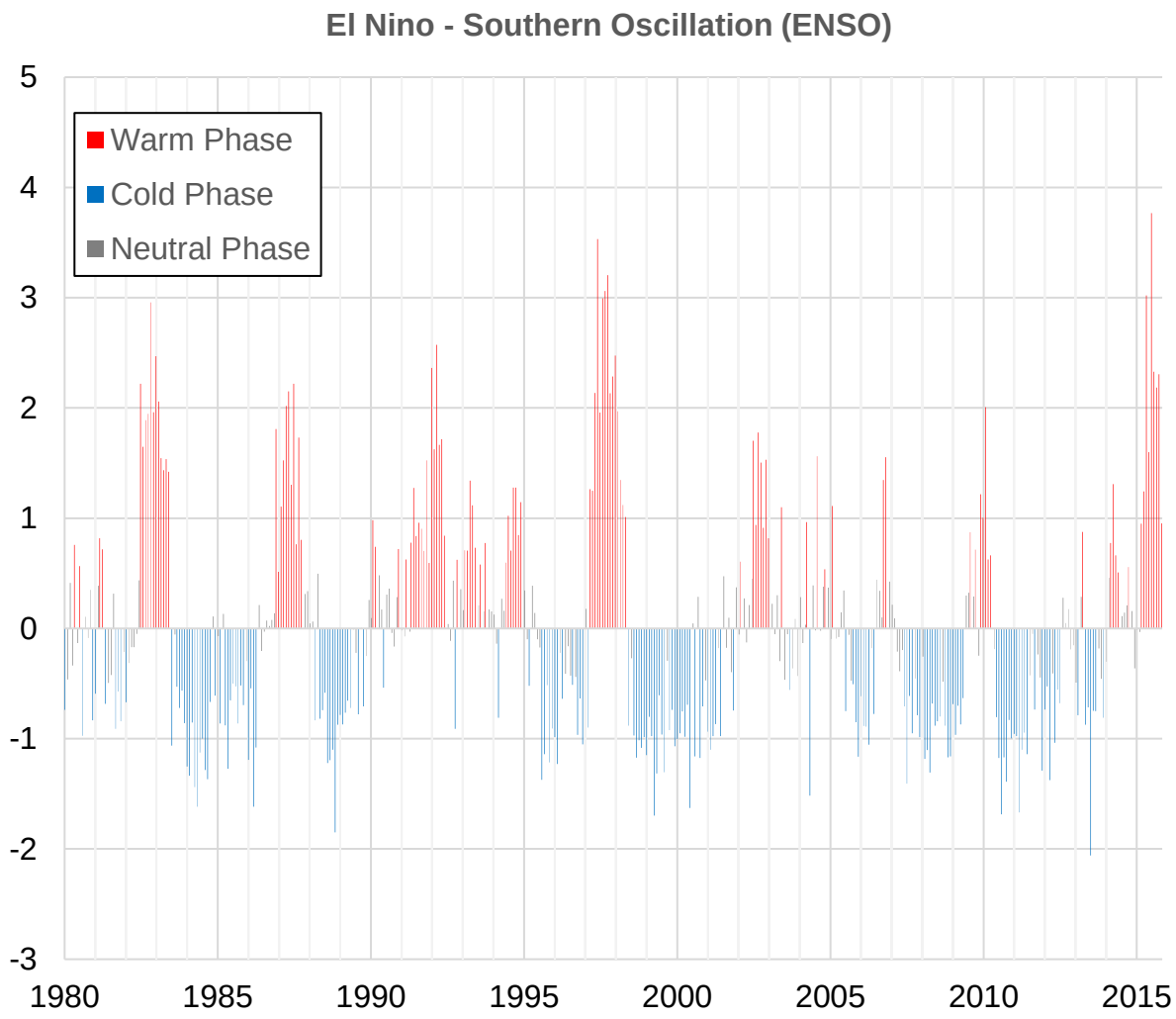

Figure 3 Graphical representation of the ENSO index, showing the various phase changes and 2-7 year cyclical pattern.

3.1.3.2. Pacific Decadal Oscillation (PDO)

The PDO time series data for 1948-2021 were retrieved from NOAA Physical Science Laboratory (Retrieved from https://psl.noaa.gov/data/climateindices/list/#PDO. Accessed 14 January 2022). SST data used in this study to create a standardized PDO index include: the UK Meteorological Office (UKMO) historical SST data set for 1900-81, Reynold's Optimally Interpolated (ROI) SST (V1) for 1982-2001, and the ROI SST V2 from 2002-present (Figure 4) (http://research.jisao.washington.edu/pdo/PDO.latest).

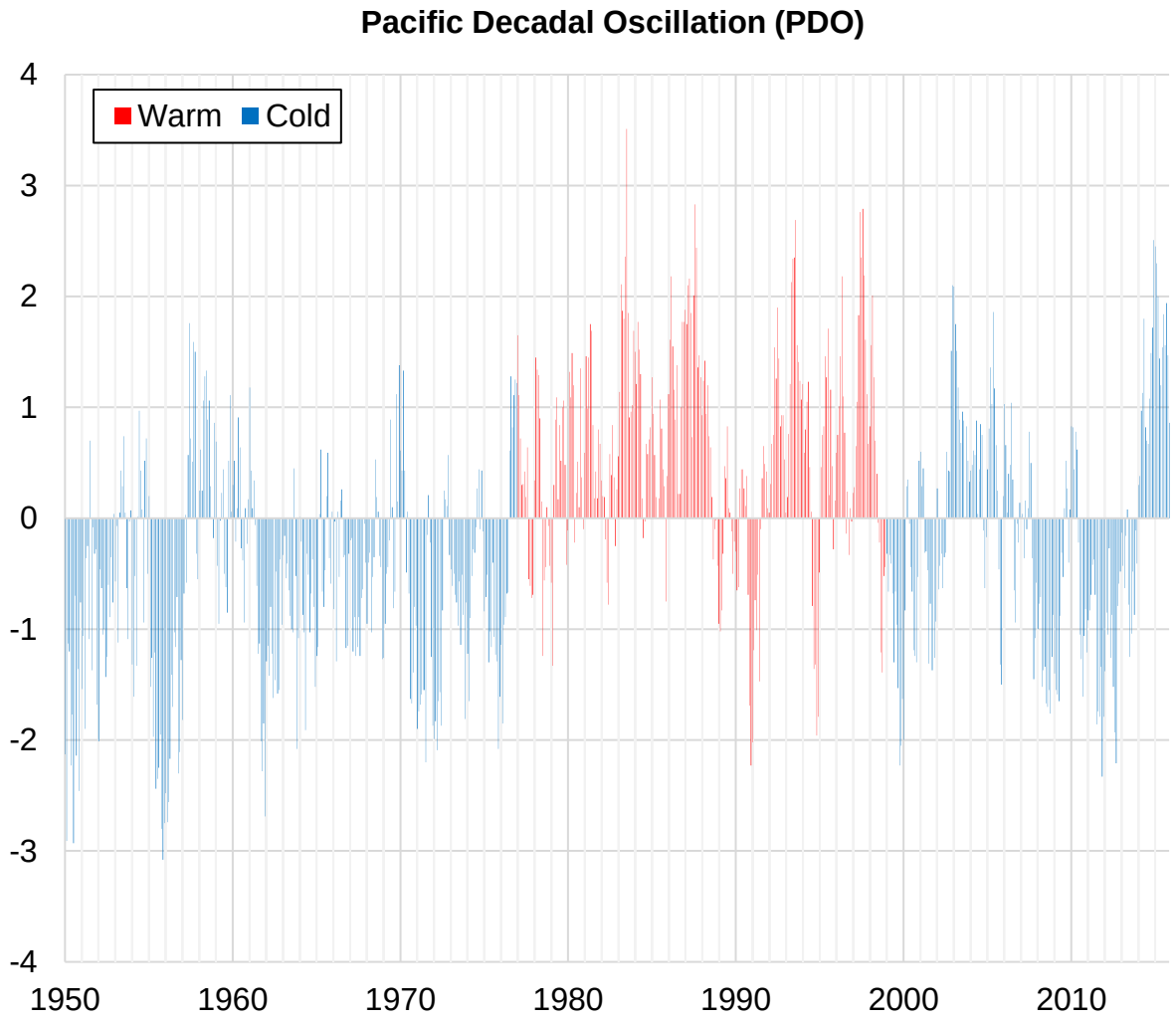

Figure 4 Graphical representation of the PDO index, showing the three phase changes and decadal pattern. The blue bars represent the PDO cold phase (1949-1976; 1999-2015) and the red bars represent the PDO warm phase (1977-1998).

3.1.3.3. North Atlantic Oscillation (NAO)

The NAO index is determined using the Rotated Principal Component Analysis [10] and time series data for 1948-2021 were retrieved from NOAA Physical Science Laboratory (Retrieved from https://psl.noaa.gov/data/climateindices/list/. Accessed 14 January 2022) (Figure 5).

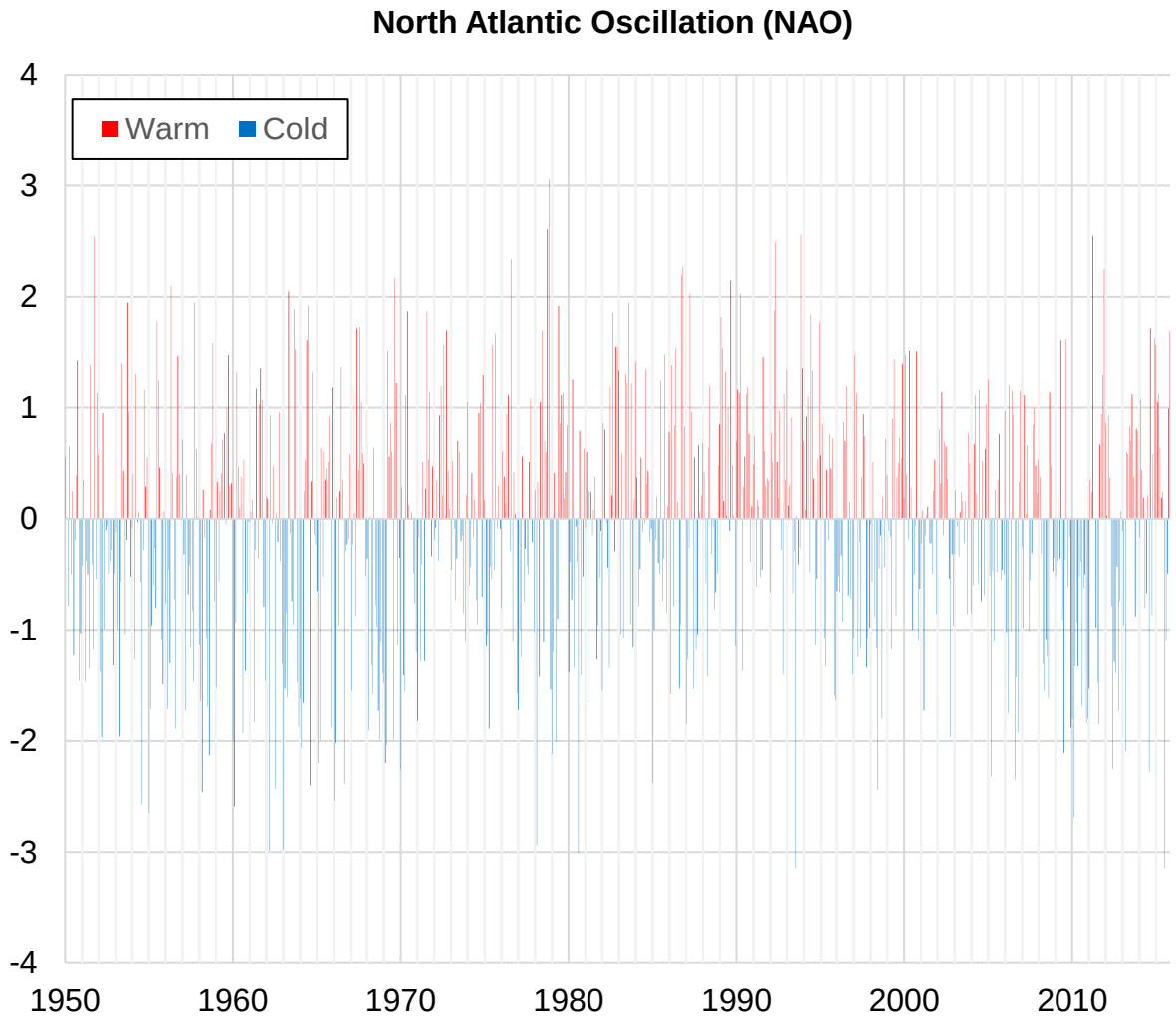

Figure 5 Graphical representation of the NAO index, showing the various phase changes and short cyclical pattern (several months to 3 years).

3.2. Methods

3.2.1. Time Series Decomposition using STL

Seasonal Trend Decomposition based on LOESS (STL) is a two-loop filter procedure that decomposes a time series into a long-term variability (including linear trend and interannual variability), seasonal, and residual components (Cleveland et al., 1990). The hydrological data (e,g, precipitation and freshwater inflows) can be described by the generative additive model as

$$Y_{hydrological\ data} = T + S + R$$

Where the T is long term variability; S is the seasonal cycle, and R is the residuals. STL analysis was done using Python™ and the STL decomposition API provided by Statsmodel (https://www.statsmodels.org/dev/api.html). The STL API has one required parameter to define the seasonal cycle in the time series, and eleven optional parameters. This API was applied to the precipitation, freshwater inflows, and climate indices (ENSO, PDO, NAO) time series. Default values for all parameters were used except for the seasonal smoother parameter. Each time series consists of monthly values; therefore, the seasonal smoother was set to 13 because it must be an odd integer.

Prior to entering the API, the long-term mean was removed from the precipitation and freshwater inflows time series to remove their anomalies. Next, each time series was entered into the STL API to decompose it to long-term variability (linear trend and interannual variability), seasonal, and residual components (Figure 6). The long-term variability was then used in the cross-correlation analysis to compare with the climate variability indices. The time span for each climate index is different and in order to

further compare the indices and precipitation/freshwater inflows, the time series needed to be the same length with the same number of data points. The precipitation and freshwater inflows time series for each bay and estuary were truncated into three separate dataframes whose time spans aligned with each climate index.

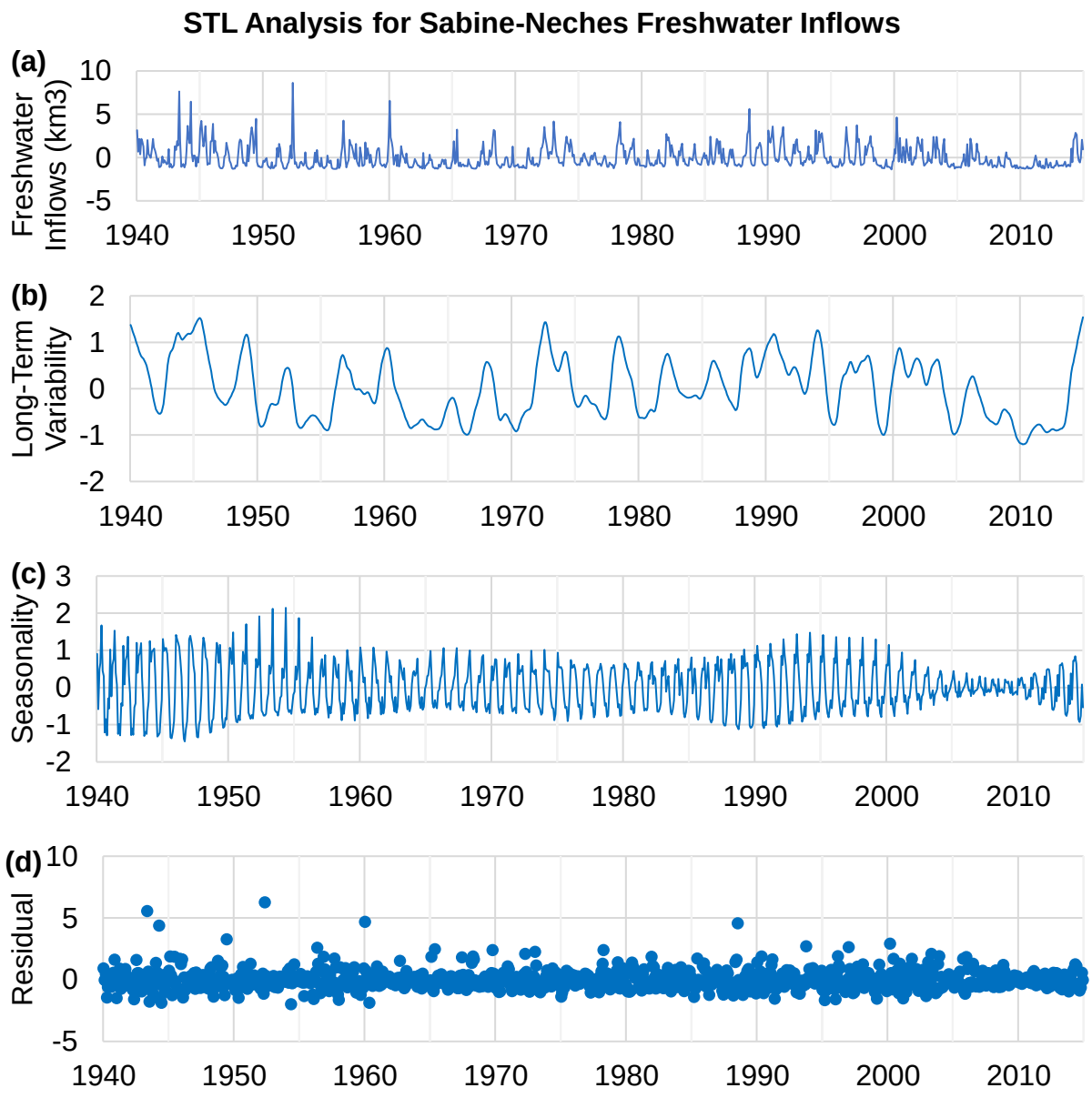

Figure 6 STL analysis results for freshwater inflows of the Sabine-Neches Estuary. The results show how the different components (long term variability, seasonality, remainder) are isolated. (a) The first panel is the freshwater inflows for the Sabine-Neches Estuary. (b) The second panel is the long-term component generated after removing the seasonal component using LOESS (c) Seasonal component, obtained by finding the recurring temporal pattern based on the seasonality value. In this analysis, seasonality was set to 13 months. (d) The residual component, which is the remaining value after the long-term variability and seasonal components were removed from the raw data. Residual values close to zero indicate less noise in the data.

3.2.2. Cross correlation analysis

Cross-correlation is used to find the relationship between two different series, and by adding a time shift, it can be used to determine if one series leads or lags the other. It is a useful technique that has often been used when observing relationships between different hydrologic cycle variables [42-44]. In this analysis, a lag of ±24 months was used and the long-term variability component for the precipitation and freshwater inflows for each estuary were cross-correlated to the long-term variability of each climate index. The climate indices were used as the independent series while the outflows and precipitation were the dependent series.

4. Results

4.1. Long-term Variability

The STL analysis allowed the long-term variability for each climate index to be isolated (Figure 7).

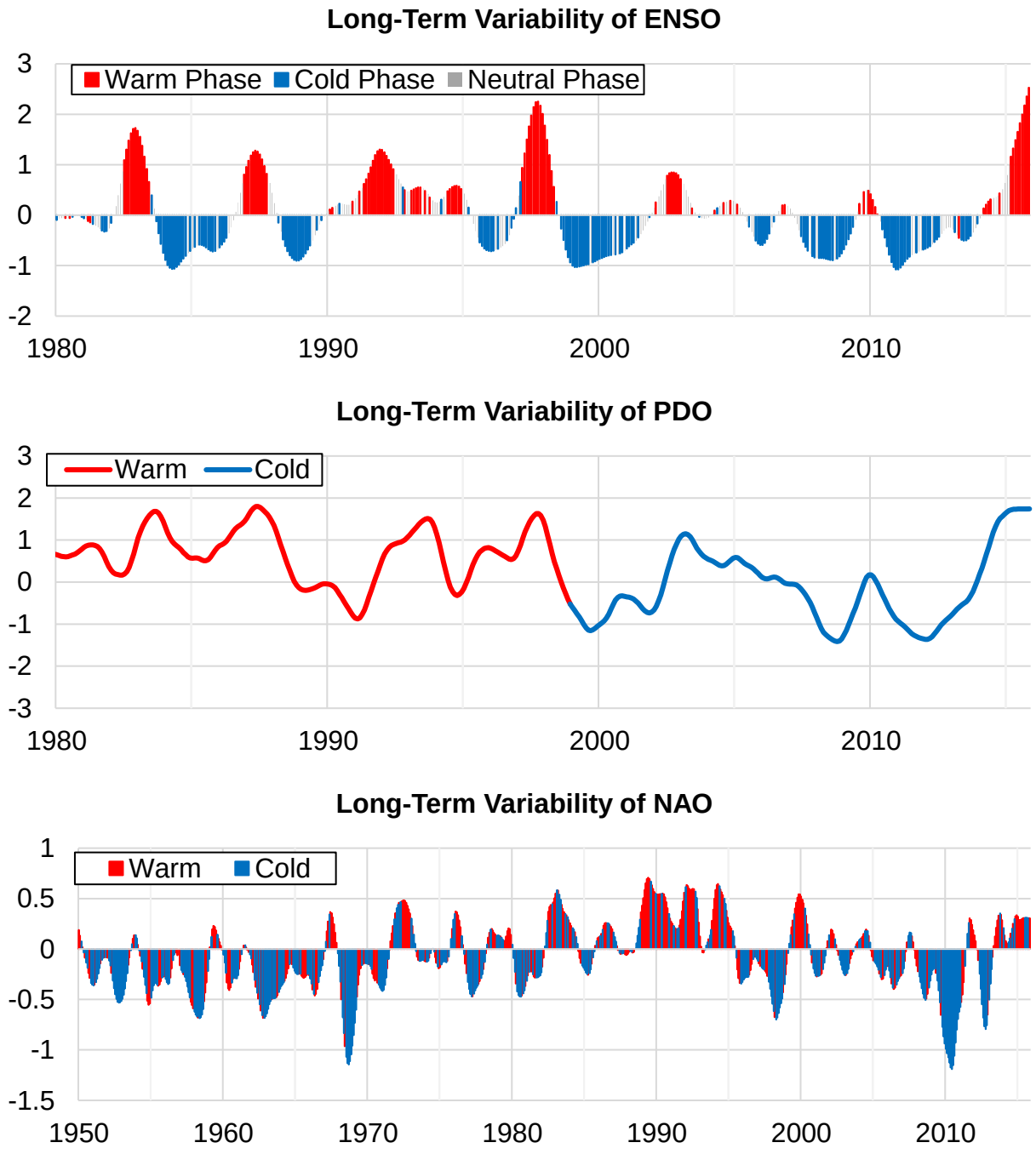

Figure 7 Isolated long-term variability for each climate index. The ENSO component clearly shows the strong El Niño events, emphasized during the PDO warm phase prior to 1998. The increased frequency and strength of La Niña event can also be seen post-1998 The PDO component shows the regime changes between cold and warm phases clearly with mostly positive values until a sharp decline in 1998 signifying the shift back to a cold phase. The NAO component shows the short cycle times of each phase with generally uniform peaks and valleys, except for one extreme low in 1968 and 2010.

The variability in the ENSO index clearly shows the El Niño and La Niña events from 1980-2015. The four peaks prior to 1998 correspond to the four recorded strong El Niño events in 1982-83, 1987-88, 1991-92, and 1997-98. These peaks also correspond to the high points in the PDO index variability. The correlation between the ENSO index and the warm phase of PDO is relatively weak (R=0.23), however the variability does show that the PDO index tends to peak during El Niño events. Post-1998, the variability shows much smaller peaks, indicating weaker El Niño events, but it also shows stronger, more sustained negative peaks, indicating stronger La Niña events in 1998-2000, 2007-08, 2011-12. In contrast to the relationship between ENSO and the warm phase of PDO, the cool phase of PDO shares a stronger correlation with ENSO (R=0.53). Like the PDO warm phase, the La Niña events correspond to the low, negative peaks in the PDO index post-1998. The variability in the NAO index shows the shorter phase cycle when compared to ENSO and PDO. It also shows a pattern similar to the phase change in PDO, with predominately positive values and seemingly longer warm phases prior to 1996. After 1996, the values are predominately negative with longer cold phases.

Next, the long-term variability for precipitation was isolated from the STL analysis (Figure 8). Despite the differences in characteristics of the estuaries, the variability shows strong similarities between them. Along the northeast Gulf coast, the Sabine-Neches and Trinity-San Jacinto exhibit remarkably similar long-term variability (R=0.82). Near the center of the coast, the Colorado-Lavaca and Guadalupe estuaries also shows a strong relationship in precipitation variability (R=0.92). The last grouping of the major estuaries has a weaker, but still relatively strong relationship. The Mission-Aransas and

Nueces estuaries are very similar (R=0.91) but the Nueces and Laguna Madre Estuaries are not as strongly related (R=0.58). However, even with the spatiotemporal difference between them, the Mission-Aransas and Laguna Madre estuaries have a moderately strong relationship (R=0.52). The first of the two minor estuaries, San Brazos and San Bernard, exhibit an extremely similar variability in precipitation (R = 0.99). The final minor estuary, East Matagorda, shares a weak relationship with the other two (R=0.34 for both). The variabilities show a decreasing amplitude in line with the climatic gradient moving from the northeast to the south, and there appear to be increase and decrease in line with El Niño and La Niña events, indicating wetter and drier periods. However, the strength of the increases and decreases do not seem to increase in magnitude depending on the phase of the PDO index.

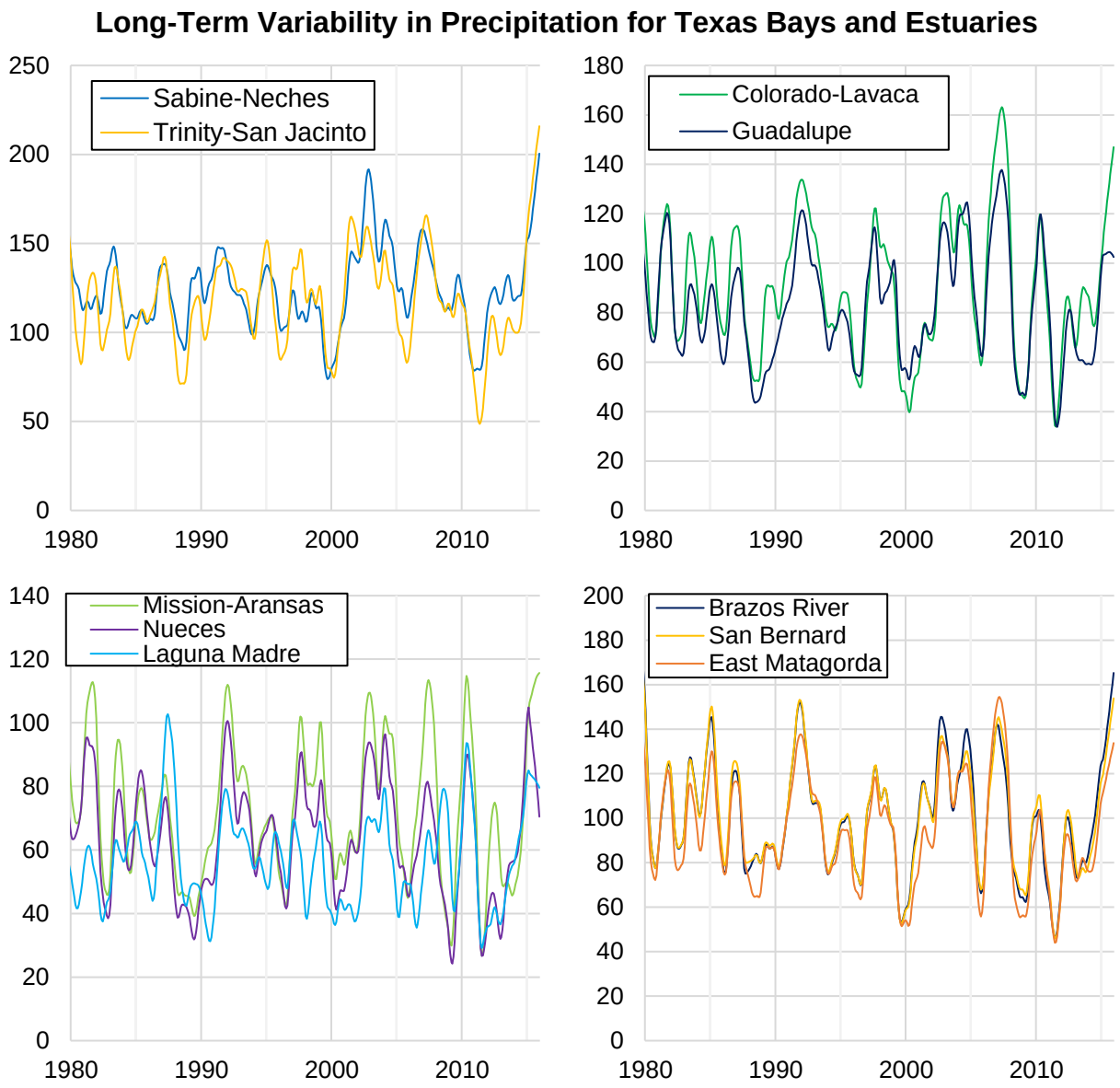

Figure 8 Long-term variability of precipitation for each estuary. The estuaries have been grouped based on similarities in variability that are seen once isolated after the STL analysis.

The isolated long-term variability for FWIs to each estuary is comparable to precipitation, with the ability to group estuaries together that share similar characteristics (Figure 9). However, the relationship between the FWIs between estuaries is not nearly as strong as seen with precipitation. Sabine-Neches and Trinity-San Jacinto Estuaries (R=0.88) and Colorado-Lavaca and Guadalupe estuaries (R=0.89) have the strongest relationship, followed by Mission-Aransas and Nueces (R=0.68) and Brazos River and San Bernard Estuaries (R=0.57). The remaining relationships between the estuary's FWI variability ranges from weak to moderate in strength (R=0.28-0.47). There does appear to be increasing and decreasing flows around the same time as El Niño and La Niña events, respectively. However, like seen in precipitation, there does not appear to be increased magnitude based on the phase of PDO (although the strong El Niño in 1991-92 corresponds to some of the higher peaks seen in the FWIs variability).

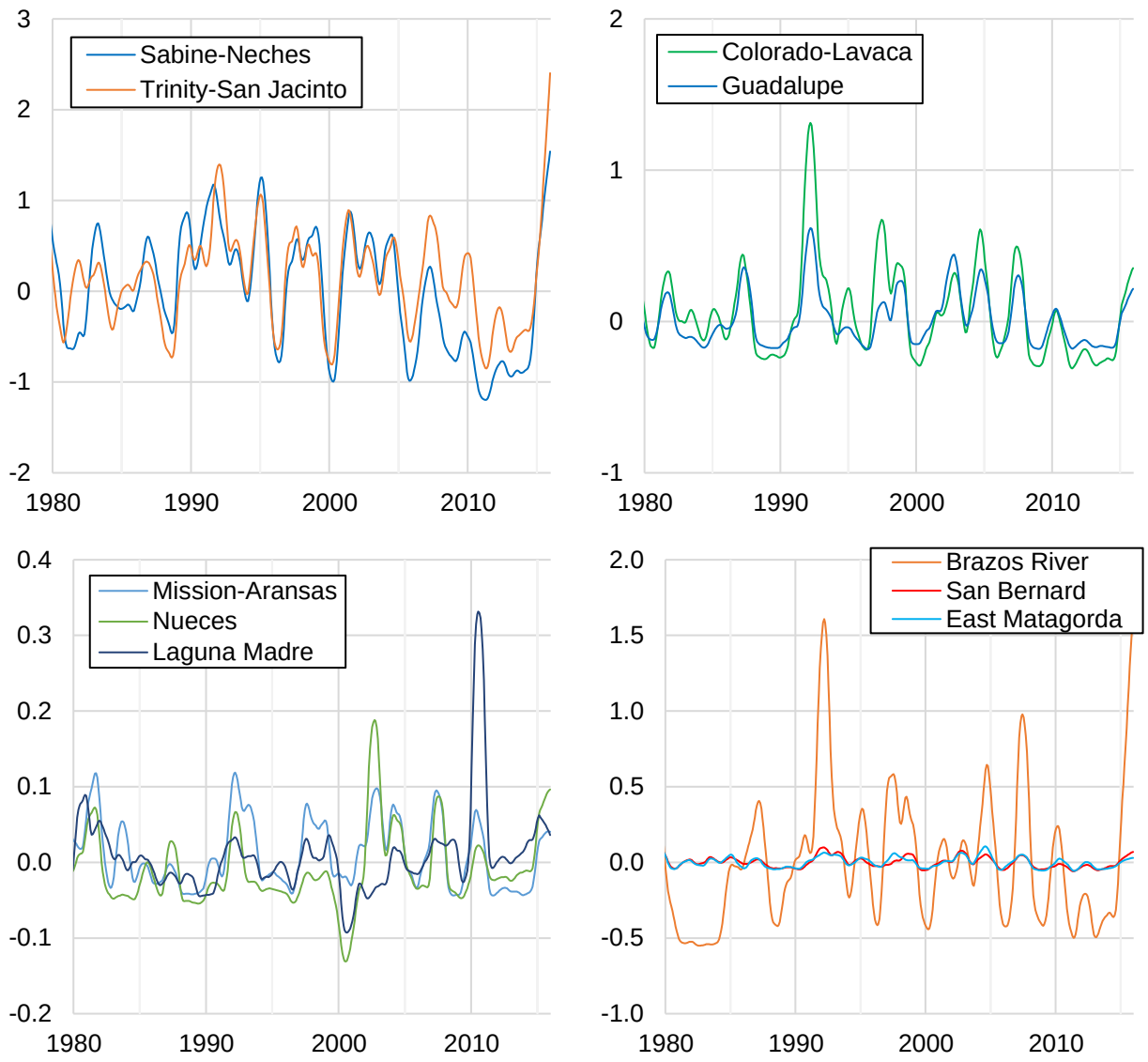

Figure 9 Long-term variability of FWIs for each estuary. The estuaries have been grouped based on similarities in variability that are seen once isolated after the STL analysis.

4.2. Correlations

4.2.1. ENSO/PDO

ENSO shows relatively strong correlations when cross-correlated with precipitation and freshwater inflows (Figure 10). The relationship was stronger between ENSO and FWIs (R=0.15-0.59; Mean=0.48) than with precipitation (R=0.37-0.54; Mean=0.47). There is a tighter lag seen with precipitation (-5 to 0 months; Mean=-2.1) than seen with freshwater inflows (-8 to 0 months; Mean=-2.4). When looking at PDO, there does not appear to be a significant relationship to the hydrology of the estuary. The relationship is moderate with precipitation (R=0.31-0.45; Mean=0.38) and freshwater inflows (R=0.12-0.48; Mean=0.33), however, there is a positive lag for both precipitation (0 to 7 months; Mean=1.7) and freshwater inflows (-5 to 4 months; Mean=1.1). This implies that the moderate relationships are not in response to variability in PDO. Because PDO is a decadal cycle and the lag is only two years, the effect of PDO on precipitation and freshwater inflows is better seen with the combined effect of PDO and ENSO.

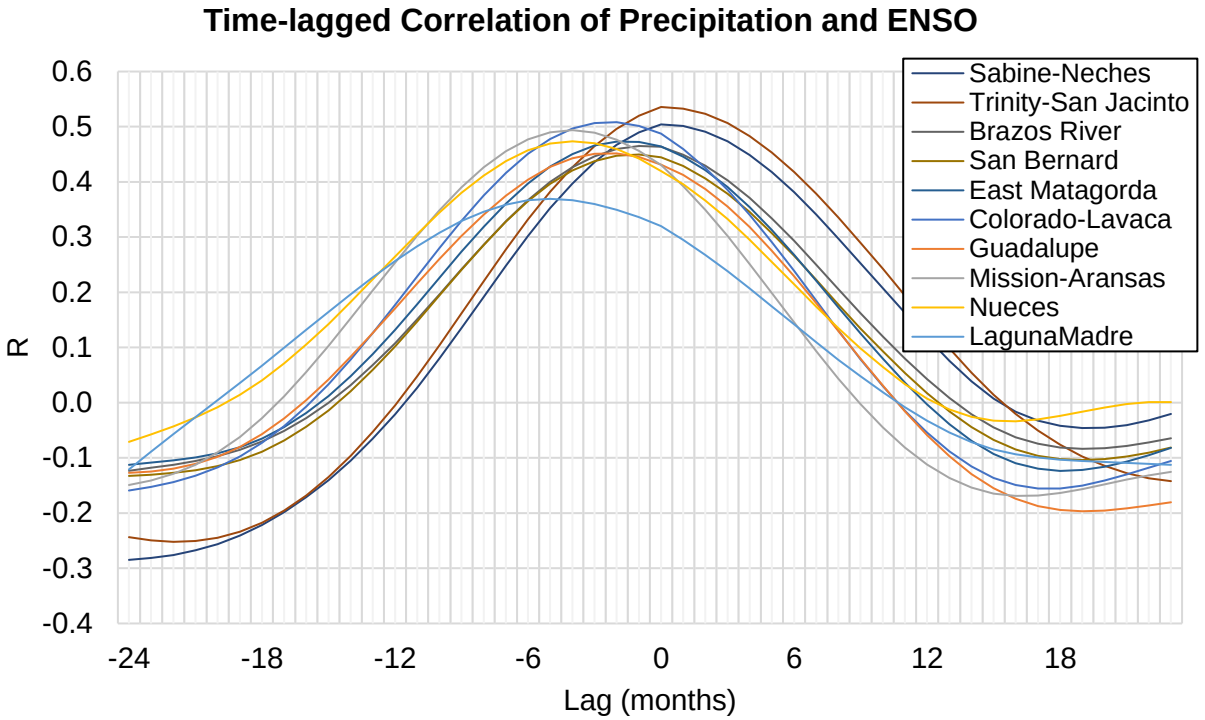

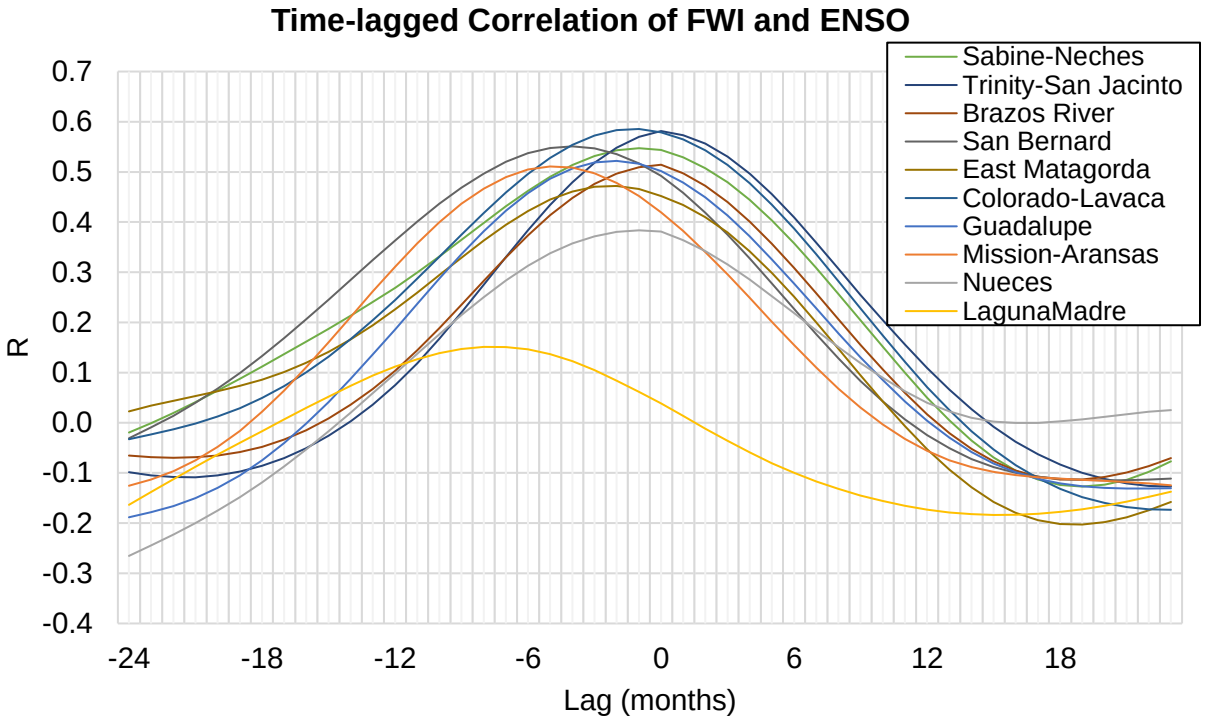

Figure 10 Cross-correlation of ENSO and precipitation/FWIs. There was a stronger correlation, on average, between ENSO and FWIs but a tighter window of lag with ENSO and precipitation.

To examine the combined effect, cross-correlations were done between ENSO, precipitation, and freshwater inflows during the PDO warm and cold phases. The relationship between ENSO and precipitation strengthens during a PDO cold phase (R=0.66-0.80; Mean=0.73) and weakens during a PDO warm phase (R=0.16-0.41; Mean = 0.29) (Figure 11). Additionally, the lag during a PDO cold phase gets longer (-7to 0 months; Mean=-3.4) and shortens during a PDO warm phase (-4 to 2 months; Mean=-1.8). The effect is the same with freshwater inflows, although less pronounced during a PDO warm phase (Figure 12). During a PDO cold phase, the relationship between FWIs and ENSO is strengthened (R=0.35-0.73; Mean=0.64) with a longer lag (-8 to 0 months; Mean=-3.5) while the relationship is slightly weakened during a PDO warm phase (R=0.19-0.51; Mean=0.39) with a shorter lag (-8 to 3 months; Mean=-1.1).

4.2.2. NAO

Cross-correlations with NAO showed much weaker relationships than both ENSO and PDO (Figure 13). The relationship between NAO and precipitation (R=0.13-0.35; Mean=0.23) was weak but does show a lag (-10 to 19 months; Mean=-6.1) consistent with a hydrologic response to driving factors from the North Atlantic. The relationship with freshwater inflows was similarly weak (R=-.20 to 0.45; Mean=0.22) and Laguna Madre estuary was the only one in the study to have a negative correlation. The time lag (-24 to 23 months; Mean=-0.3) also did not represent a hydrologic response to NAO.

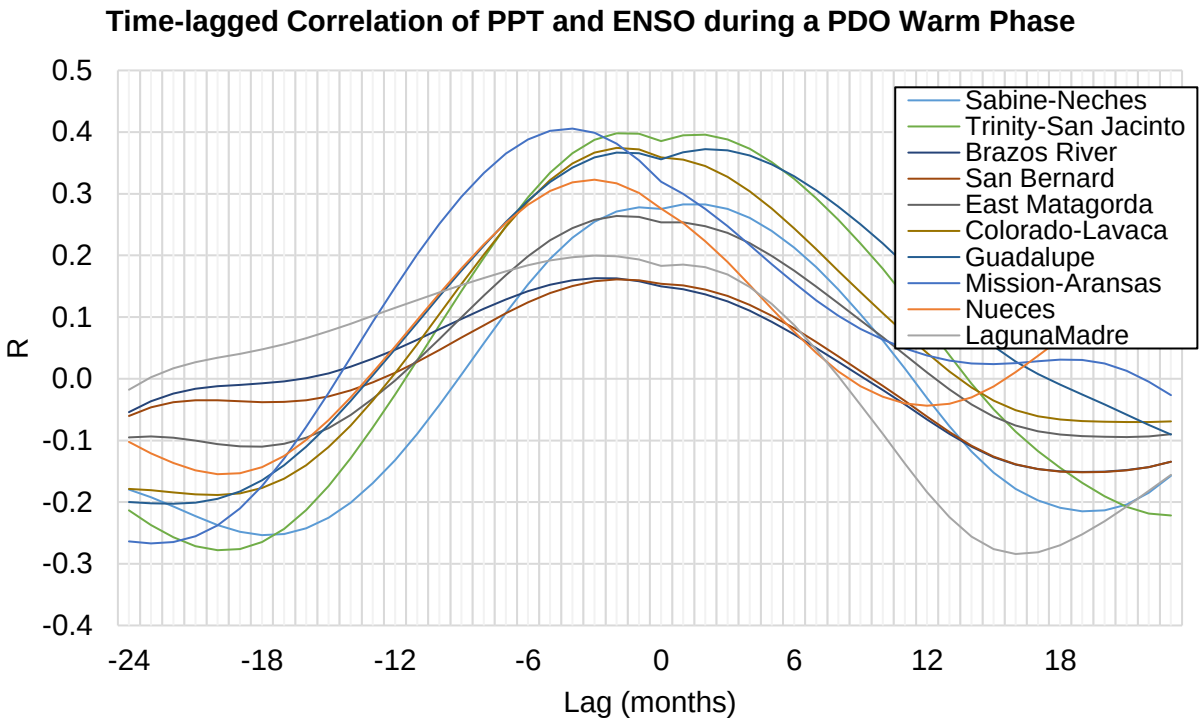

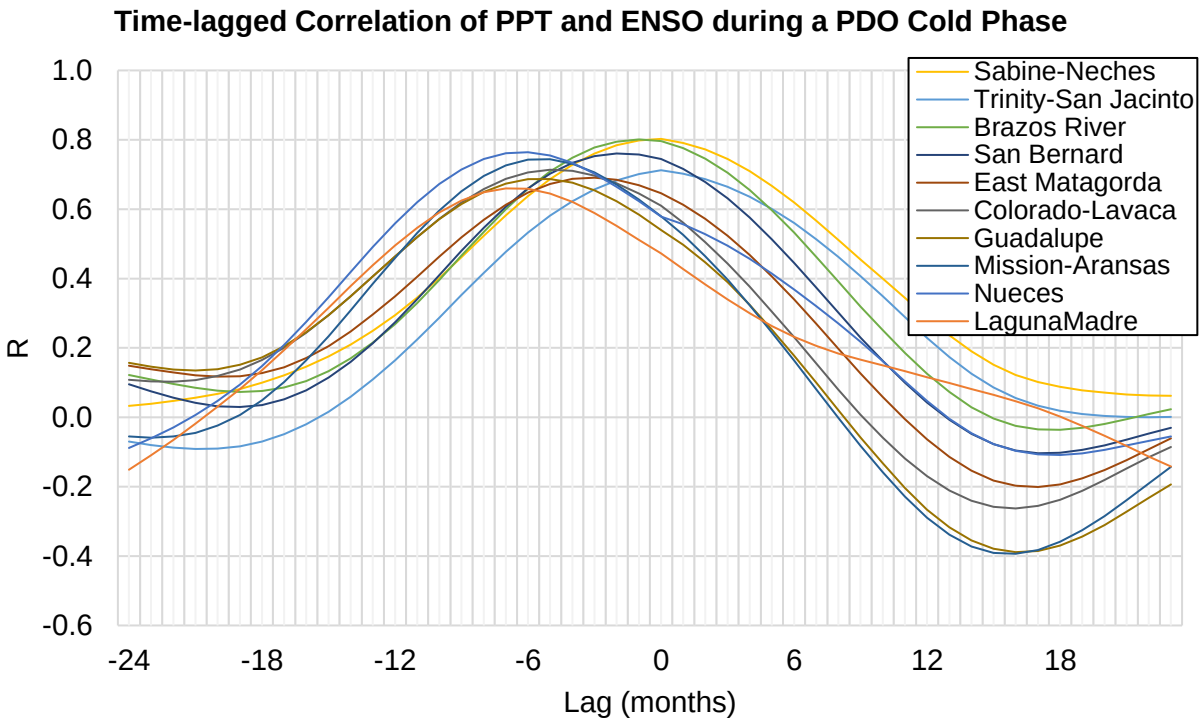

Figure 11 Time-lagged correlation between ENSO and precipitation during a PDO warm and cold phase. The relationship is strengthened during a cold phase and weakened during a warm phase.

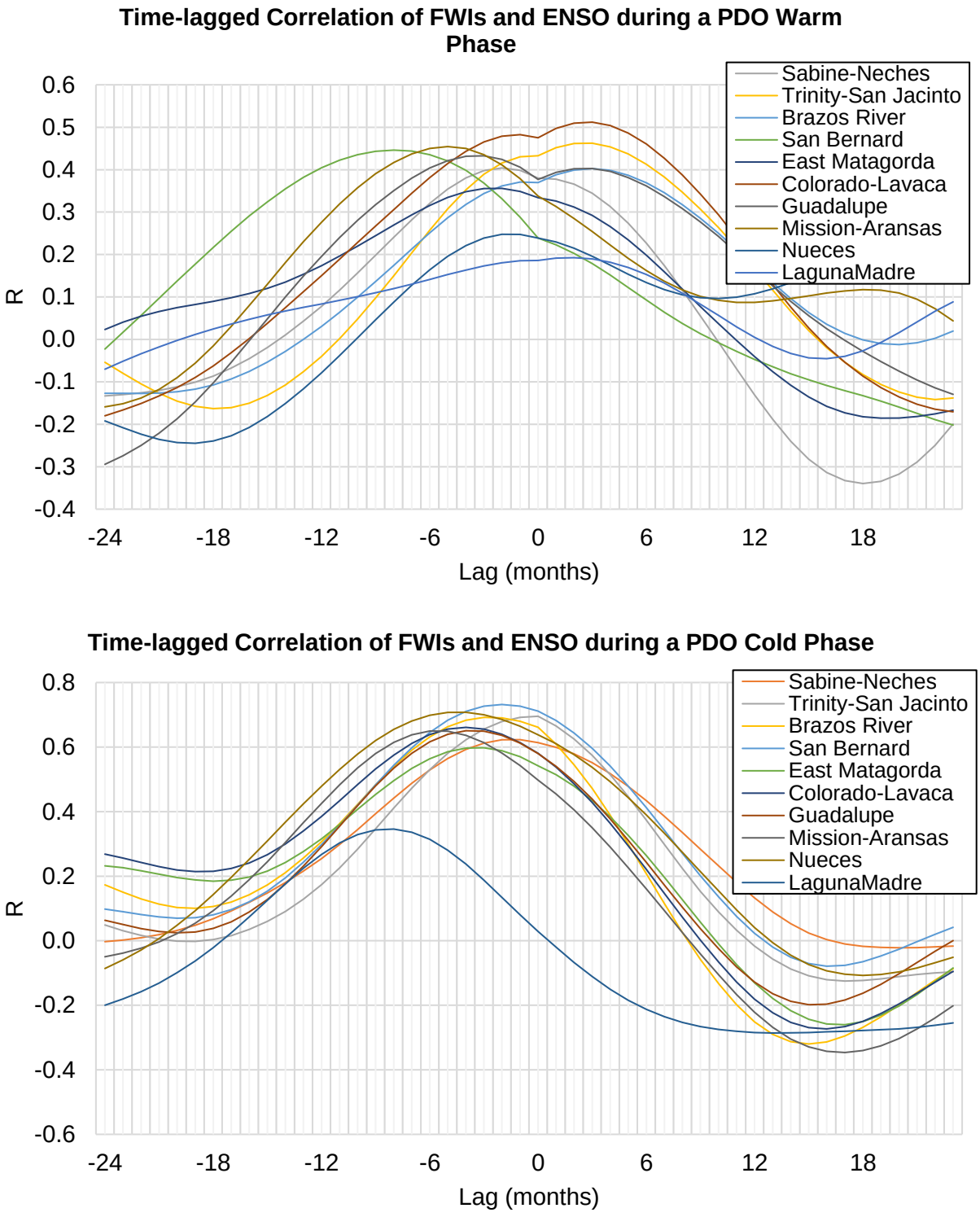

Figure 12 Time-lagged correlation between ENSO and FWIs during a PDO warm and cold phase. The relationship is strengthened during a cold phase and weakened during a warm phase.

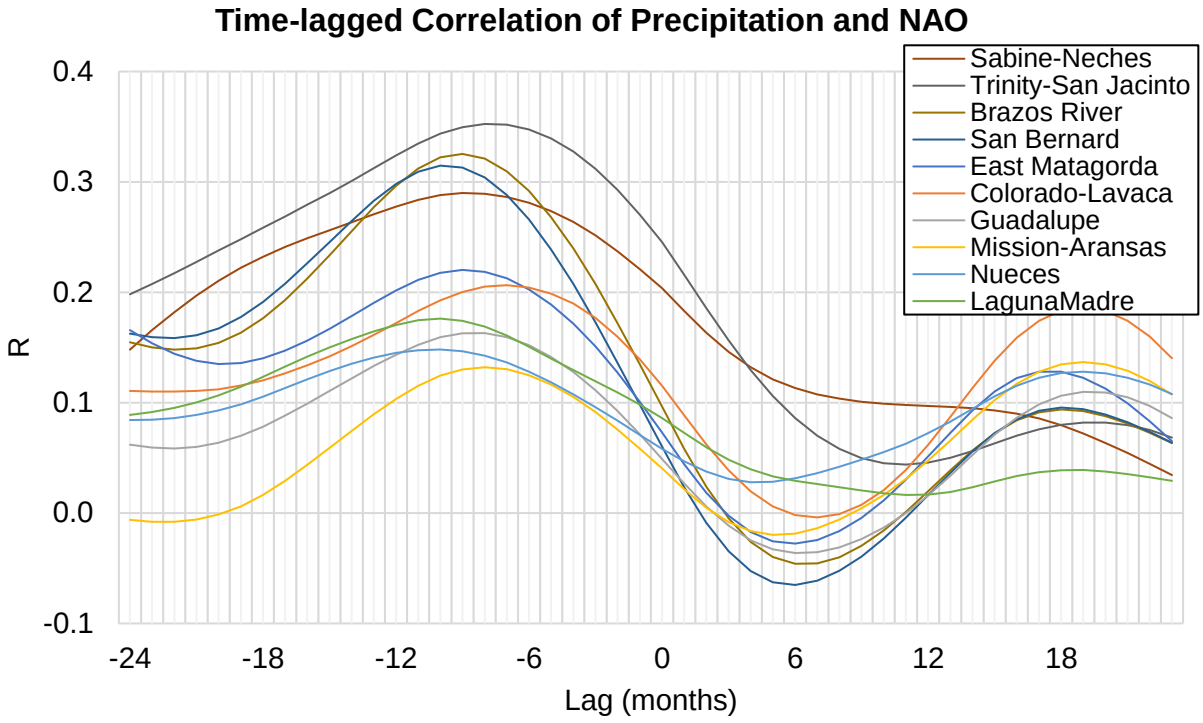

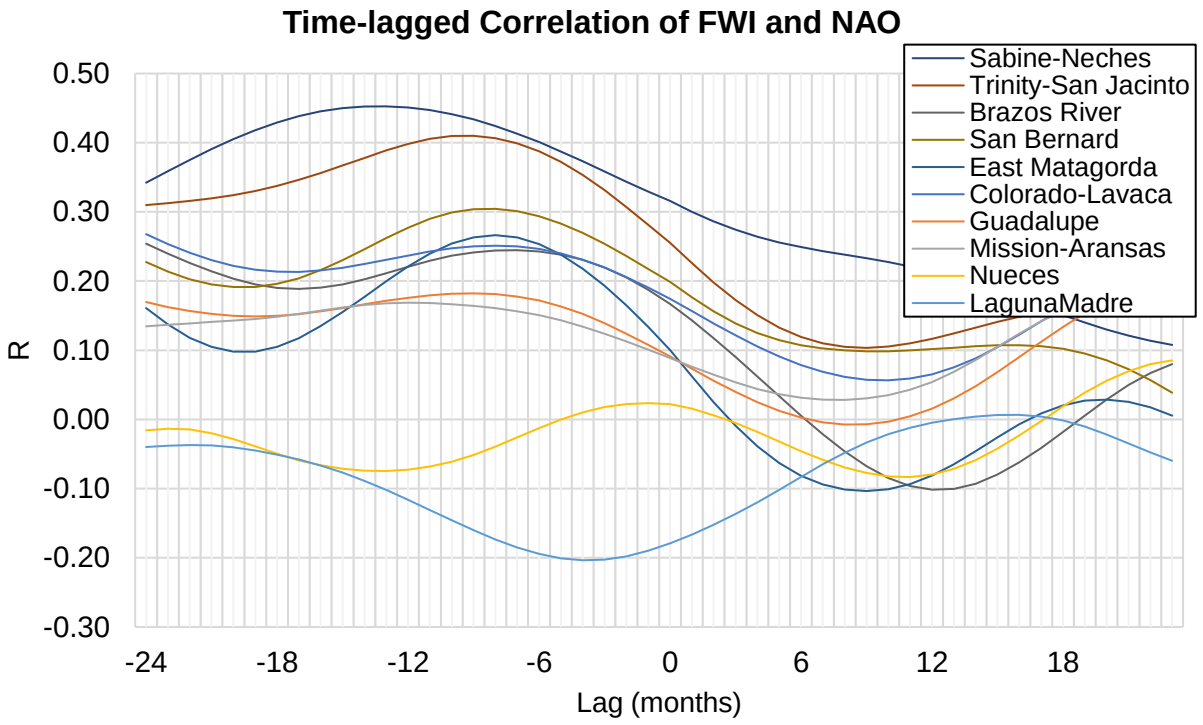

Figure 13 Time-lagged correlation between NAO, precipitation, and FWIs. It shows a much weaker relationship than seen with the other climate indices and only the relationship with precipitation indicates a hydrological response to driving factors of NAO.

5. Conclusions

5.1. Cross-Correlations of Precipitation

	ENSO		PDO		NAO	
	R	**Lag**	**R**	**Lag**	**R**	**Lag**
Sabine-Neches	0.50	0	0.31	7	0.29	-9
Trinity-San Jacinto	0.54	0	0.37	1	0.35	-8
Brazos	0.47	-1	0.45	2	0.33	-7
San Bernard	0.45	-1	0.43	1	0.32	-8
East Matagorda	0.47	-2	0.41	2	0.22	-9
Colorado-Lavaca	0.51	-2	0.38	0	0.21	-7
Guadalupe	0.45	-2	0.36	0	0.16	-8
Mission-Aransas	0.49	-4	0.37	0	0.14	19
Nueces	0.7	-4	0.4	1	0.15	-10
Laguna Madre	0.37	-5	0.35	0	0.18	-10

Table 1 Results of cross-correlation of climate indices and precipitation for each estuary. The correlation column shows the strongest correlation, and the lag column shows the corresponding lag, in months, the correlation occurred.

ENSO showed stronger correlations with precipitation than the other two indices. Only Laguna Madre had an R-value lower than 0.45. When the long-term variability of precipitation was observed for each basin, they were able to be grouped by similar variability patterns. This grouping carried into the correlations with similar strengths between the grouped estuaries. Additionally, the observed lags were almost identical among the groups, with a lag of 0 months in the northeast estuaries (Sabine-Neches and Trinity-San Jacinto), -2 months for the central estuaries (Colorado-Lavaca and

Guadalupe) and -5 to -4 for the southern estuaries (Mission-Aransas, Nueces, and Laguna Madre). The minor estuaries also had similar lags of -2 to -1 months.

	Cold PDO		Warm PDO	
	R	**Lag**	**R**	**Lag**
Sabine-Neches	0.80	0	0.28	1
Trinity-San Jacinto	0.71	0	0.40	-2
Brazos	0.80	-1	0.16	-3
San Bernard	0.76	-2	0.16	-2
East Matagorda	0.69	-3	0.26	-2
Colorado-Lavaca	0.71	-5	0.37	-2
Guadalupe	0.69	-5	0.37	2
Mission-Aransas	0.74	-5	0.41	-4
Nueces	0.76	-6	0.32	-3
Laguna Madre	0.66	-7	0.20	-3

Table 2 Cross-correlations between precipitation and ENSO during a cold and warm phase of PDO

PDO showed similar patterns of correlation as ENSO, albeit weaker, with the major estuaries having moderate positive correlations (R=0.31-0.45). However, most of the lags are positive (1-7 months) with four estuaries having no lag. This does not represent a response to driving factors of PDO and as mentioned previously, the effect of PDO can be seen in the combined effects of PDO and ENSO (Table 2). During a cold PDO phase, the strength of the ENSO-precipitation relationship significantly increases, while the opposite is true for a warm PDO phase.

NAO had very weak positive relationships with precipitation. The Trinity-San Jacinto Estuary had the strongest relationship when a lag is applied (R = 0.35), but it is much lower than the relationship seen with the freshwater inflows. The lag followed a much more consistent pattern, however, with nine of the 10 estuaries seeing their strongest relationships between -10 and -7 months.

5.2. Cross-Correlations of Freshwater Inflows

	ENSO		PDO		NAO	
	R	**Lag**	**R**	**Lag**	**R**	**Lag**
Sabine-Neches	0.55	-1	0.33	0	0.45	-13
Trinity-San Jacinto	0.58	0	0.42	1	0.41	-9
Brazos	0.51	0	0.25	0	0.25	-24
San Bernard	0.55	-4	0.41	3	0.30	-8
East Matagorda	0.47	-2	0.37	3	0.27	-8
Colorado-Lavaca	0.59	-1	0.48	2	0.27	-24
Guadalupe	0.52	-2	0.36	2	0.19	23
Mission-Aransas	0.51	-5	0.37	1	0.18	21
Nueces	0.38	-1	0.12	4	0.09	23
Laguna Madre	0.15	-8	0.17	-5	-0.20	16

Table 3 Results of cross-correlation of climate indices and freshwater inflows for each estuary. The correlation column shows the strongest correlation, and the lag column shows the corresponding lag, in months, the correlation occurred.

The cross-correlation analysis on freshwater inflows yielded very similar results to the precipitation analysis. ENSO shows the strongest positive correlations when compared to the other two climate indices. Again, PDO does not seem to have a significantly strong relationship with freshwater inflows independently. When combined with ENSO,

the relationships get stronger during a cold PDO phase and weaker during a warm PDO phase (Table 4). Finally, NAO shows a moderately strong positive relationship with the freshwater inflows to the estuaries in the northeast (Sabine-Neches and Trinity-San Jacinto). With NAO shown to influence the hydrologic cycle in the eastern United States, this relationship points to a moderate response in the northeast Gulf to driving factors in the Atlantic Ocean brought on by NAO.

	Cold PDO		**Warm PDO**	
	R	**Lag**	**R**	**Lag**
Sabine-Neches	0.62	-1	0.40	-2
Trinity-San Jacinto	0.70	0	0.46	3
Brazos	0.69	-3	0.40	3
San Bernard	0.73	-2	0.45	-8
East Matagorda	0.60	-3	0.36	-2
Colorado-Lavaca	0.66	-4	0.51	3
Guadalupe	0.65	-4	0.43	-3
Mission-Aransas	0.65	-6	0.45	-5
Nueces	0.71	-4	0.25	-2
Laguna Madre	0.35	-8	0.19	2

Table 4 Cross-correlations between FWIs and ENSO during a cold and warm phase of PDO

5.3. Conclusions

This study focused on assessing the relationship between the local hydrology of the estuaries in Texas and the regional to global climate variability in the Pacific and Atlantic Oceans. Results show that there are moderately strong positive correlations between

ENSO and precipitation (R = 0.37 to 0.70) with mostly higher precipitation during El Niño and lower precipitation during La Niña. These correlations were weakened during PDO warm phase (R = 0.16 to 0.41) and amplified during PDO cool phase (R = 0.69 to 0.8). Temporal variability in precipitation was linked to bay and estuary freshwater inflows, showing high flows during El Nino and low flows during La Nina. Additionally, there are moderately strong positive correlations between NAO and freshwater inflows to two of the 10 bays/estuaries in the northeast (Sabine-Neches and Trinity San Jacinto, R = 0.45 and 0.41). These correlations tend to occur within the year of the driving conditions in the Pacific and Atlantic Oceans. Identifying these linkages and the corresponding response times can help predict the hydrologic response to wet and dry climate cycles linked to climate teleconnections along the Texas Gulf Coast and inform management strategies to help protect and maintain the health of the vital estuarine environments.

References

1. Tolan, J.M., *El Niño-Southern Oscillation impacts translated to the watershed scale: Estuarine salinity patterns along the Texas Gulf Coast, 1982 to 2004.* Estuarine, Coastal and Shelf Science, 2007. **72**(1): p. 247-260.
2. Pollack, J., T. Palmer, and P. Montagna, *Long-term trends in the response of benthic macrofauna to climate variability in the Lavaca-Colorado Estuary, Texas.* Marine Ecology Progress Series, 2011. **436**: p. 67-80.
3. Kim, H.-C., et al., *Linkage between Freshwater Inflow and Primary Productivity in Texas Estuaries: Downscaling Effects of Climate Variability.* Journal of coastal research, 2014. **68**(sp1): p. 65-73.
4. Alber, M., *A Conceptual Model of Estuarine Freshwater Inflow Management.* Estuaries, 2002. **25**(6): p. 1246-1261.
5. Barlow, M., S. Nigam, and E. Berbery, *ENSO, Pacific Decadal Variability, and U.S. Summertime Precipitation, Drought, and Stream Flow.* Journal of Climate, 2001. **14**: p. 2105-2128.
6. Gershunov, A. and T.P. Barnett, *Interdecadal Modulation of ENSO Teleconnections.* Bulletin of the American Meteorological Society, 1998. **79**(12): p. 2715-2725.
7. Goodrich, G.B., *Influence of the Pacific Decadal Oscillation on Winter Precipitation and Drought during Years of Neutral ENSO in the Western United States.* Weather and Forecasting, 2007. **22**(1): p. 116-124.
8. Mantua, N.J., et al., *A Pacific Interdecadal Climate Oscillation with Impacts on Salmon Production*.* Bulletin of the American Meteorological Society, 1997. **78**(6): p. 1069-1080.
9. Moore, C., *Pacific Decadal Oscillation and Southern United States Climate*. 2021, Climate Institute: Washington, DC.
10. Barnston, A.G. and R.E. Livezey, *Classification, Seasonality and Persistence of Low-Frequency Atmospheric Circulation Patterns.* Monthly Weather Review, 1987. **115**(6): p. 1083-1126.
11. Wallace, J.M. and D.S. Gutzler, *Teleconnections in the Geopotential Height Field during the Northern Hemisphere Winter.* Monthly Weather Review, 1981. **109**(4): p. 784-812.
12. Lindsey, R., Dahlman, Luann. *Climate Variability: North Atlantic Oscillation*. 2021 2021; Available from: https://www.climate.gov/news-features/understanding-climate/climate-variability-north-atlantic-oscillation.
13. Chartrand, J. and F.S.R. Pausata, *Impacts of the North Atlantic Oscillation on winter precipitations and storm track variability in southeast Canada and the northeast United States.* Weather Clim. Dynam., 2020. **1**(2): p. 731-744.
14. Warren, R.J. and M.A. Bradford, *Seasonal Climate Trends, the North Atlantic Oscillation, and Salamander Abundance in the Southern Appalachian Mountain Region.* Journal of Applied Meteorology and Climatology, 2010. **49**(8): p. 1597-1603.
15. Myoung, B., et al., *On the Relationship between the North Atlantic Oscillation and Early Warm Season Temperatures in the Southwestern United States.* Journal of Climate, 2015. **28**(14): p. 5683-5698.

16. Slade Jr, R.M. and T.E. Chow, *Statistical relations of precipitation and stream runoff for El Niño and La Niña periods, Texas Hill Country.* Texas Water Journal, 2011. **2**(1): p. 1-22.
17. Wei, W. and D.W. Watkins, Jr, *Probabilistic streamflow forecasts based on hydrologic persistence and large-scale climate signals in central Texas.* Journal of Hydroinformatics, 2010. **13**(4): p. 760-774.
18. Johns, N.D., Hess, Myron, Kaderka, Susan, McCormick, Lacey, McMahon, Jennifer, *Bays in Peril: A Forecast for Freshwater Flows to Texas Estuaries*. 2004, National Wildlife Federation. p. 48.
19. Rosen, R., *Bays and Estuaries*, in *Texas Aquatic Science*. 2022, Texas A&M University Press.
20. Group, E.T.R.W.P., *East Texas Regional Water Planning Area 2021 Regional Water Plan*. 2020. p. 472.
21. *Freshwater Inflow Recommendation for the Sabine Lake Estuary of Texas and Louisiana*. 2005, Texas Parks and Wildlife Department: Austin, TX. p. 75.
22. Guthrie, C.G., Matsumoto, J., and Solis, R.S., *Analysis of the Influence of Water Plan Strategies on Inflows and Salinity in Galveston Bay*, in *Final report to the United States Army Corps of Engineers, Contract #R0100010015*. 2012: Texas Water Development Board, Austin, TX. p. 71.
23. Guthrie, C.G., Lu, Qingguang, Schoenbaechler, C., *Coastal Hydrology for the Trinity-San Jacinto Estuary*. 2012, Texas Water Development Board: Austin, TX. p. 29.
24. Guthrie, C.G., Lu, Qingguang, Matsumoto, Junji, Negusse, Solomon, Schoenbaechler, Caimee, *TxBLEND Model Calibration and Validation for the Lavaca-Colorado Estuary and East Matagorda Bay*. 2011, Texas Water Development Board: Austin, TX. p. 72.
25. Guthrie, C.G., Lu, Qingguang, Schoenbaechler, C., *Coastal Hydrology for the Lavaca-Colorado Estuary*. 2011, Texas Water Development Board: Austin, TX. p. 18.
26. *Matagorda Bay Freshwater Inflow Needs Study*. 2006, Lower Colorado River Authority, Texas Commission on Environmental Quality, Texas Parks and Wildlife, Texas Water Development Board. p. 280.
27. Guthrie, C.G., Matsumoto, J., and Lu, Qingguang, *TxBLEND Model Calibration and Validation for the Guadalupe and Mission-Aransas Estuaries*. 2010, Texas Water Development Board: Austin, TX. p. 46.
28. Slack, R.D., Grant, William E., Davis III, Stephen E., Swannack, Todd M., Wozniak, Jeffrey, Greer, Danielle, Snelgrove, Amy, *Linking Freshwater Inflows and Marsh Community Dynamics in San Antonio Bay to Whooping Cranes*. 2009, Guadaluoe Blanco River Authority, San Antonio River Authority. p. 187.
29. Veatch, B., *2021 South Central Texas Regional Water Plan*. 2020, South Central Texas Regional Water Planning Group. p. 656.
30. Chen, G.F., *Freshwater Inflow Recommendation for the Mission-Aransas Estuarine System*. 2010, Texas Parks and Wildlife Department: Austin, TX. p. 131.
31. Evans, A., Madden, Kiersten, Palmer, Sally, *The Ecology and Sociology of the Mission-Aransas Estuary: An Estuarine and Watershed Profile*. 2012.

32. Erin, M.H., A.N. Brien, and V.Z. Paul, *History of Water and Habitat Improvement in the Nueces Estuary, Texas, USA.* Texas water journal, 2011. **2**(1).
33. Schoenbaechler, C., Guthrie, Carla G., Lu, Qingguang, *Coastal Hydrology for the Nueces Estuary: Hydrology for Version #TWDB201101 with Updates to Diversion and Return Data for 2000-2009*. 2011, Texas Water Development Board: Austin, TX.
34. Schoenbaechler, C., Guthrie, Carla G., Matsumoto, Junji, Lu, Qingguang, *TxBLEND Model Calibration and Validation for the Laguna Madre Estuary*. 2011, Texas Water Development Board: Austin, TX. p. 60.
35. Schoenbaechler, C., Guthrie, Carla G., Lu, Qingguang, *Coastal Hydrology for the Laguna Madre Estuary, with Emphasis on the Lower Laguna Madre*. 2011, Texas Water Development Board: Austin, TX. p. 29.
36. Schoenbaechler, C., Guthrie, Carla G., Lu, Qingguang, *Coastal Hydrology for the Brazos River Estuary*. 2011, Texas Water Development Board: Austin, TX. p. 13.
37. *San Bernard River and Cedar Lakes Estuary*. Available from: https://www.twdb.texas.gov/surfacewater/bays/minor_estuaries/san_bernard/index.asp.
38. *East Matagorda Bay*. Available from: https://www.twdb.texas.gov/surfacewater/bays/minor_estuaries/east_matagorda/index.asp.
39. Group, P.C. 2014, Oregon State University.
40. Daly, C., G. Taylor, and W. Gibson, *The PRISM Approach to Mapping Precipitation and Temperature.* 1997.
41. Curtis, S. and R. Adler, *ENSO Indices Based on Patterns of Satellite-Derived Precipitation.* Journal of Climate, 2000. **13**(15): p. 2786-2793.
42. Clark, C., II, G.A. Nnaji, and W. Huang, *Effects of El-Niño and La-Niña Sea Surface Temperature Anomalies on Annual Precipitations and Streamflow Discharges in Southeastern United States.* Journal of Coastal Research, 2014. **SI**(68): p. 113-120.
43. Seo, S.B., et al., *The role of cross-correlation between precipitation and temperature in basin-scale simulations of hydrologic variables.* Journal of Hydrology, 2019. **570**: p. 304-314.
44. Zhang, Z., et al., *Evaluating the non-stationary relationship between precipitation and streamflow in nine major basins of China during the past 50years.* Journal of Hydrology, 2011. **409**(1): p. 81-93.